# Chapter 3

# Finite Element Formulation

For solving the equations describing the diaphragm deformation we will use the finite element method. In this chapter we will present the formulation of the method for geometrically nonlinear, three-dimensional continuum elements. We will focus on the particular aspect of rubber-like materials. The basic ideea of the nonlinear finite element formulation is to linearize the *weak* form of the equations of the problem and to solve these equations for the finite elements discretized domain. This leads to an incremental approach, the solution at each *step* being obtained from the solution at the previous *step*. By *step* it is understood a *load increment* in static analysis, and, a *time step* in transient analysis [12][58]. In solid mechanics the *weak form* form is usualy derived from the *principle of virtual work*. In our presentation for the weak and linearized form we follow the formulation given by Simo and Taylor [50]. For the finite element implementation we use a similar approach as used by Schweizerhof [46] and Bathe [12]. The time integration scheme and the numerical algorithms are described according to [27][28] and [1]-[4].

## 3.1 Weak formulation

Following Simo and Taylor [50] let

$$T_{\mathcal{C}} = \left\{ \boldsymbol{v} : \Omega \longrightarrow \mathbf{R}^3 \mid \ \boldsymbol{v} \circ \boldsymbol{\chi}|_{\Sigma_u} = 0 \right\},$$

be the linear space of all admissible variations $\boldsymbol{v}$ in the present configuration. In the classical notation $\boldsymbol{v}$ stands for $\delta \boldsymbol{u}$. The principle of virtual work written in the present configuration states that for an arbitrary admissible variation $\boldsymbol{v} \in T_{\mathcal{C}}$

$$D_{\boldsymbol{\chi}} \mathcal{L} \cdot \boldsymbol{v} = \int_{\Omega} \boldsymbol{\sigma} : \bigtriangledown^s \boldsymbol{v} \, d\Omega - \int_{\Sigma} \boldsymbol{t} \cdot \boldsymbol{v} \, d\Sigma + \int_{\Omega} \rho \ddot{\boldsymbol{U}} \cdot \boldsymbol{v} \, d\Omega = 0, \tag{3.1}$$

where $D_{\boldsymbol{\chi}}[\ ] \cdot \boldsymbol{v}$ represents the Gateaux derivative at $\boldsymbol{\chi}$ in the direction $\boldsymbol{v}$, $\bigtriangledown^s$ is defined in (2.31) and $\boldsymbol{t} = \boldsymbol{\sigma} \cdot \boldsymbol{n}$ represents the tractions. Using (2.14) and the formulae from section 3.6, the equation (3.1) can be written consecutively

$$\int_{\Omega_R} \frac{1}{J} \boldsymbol{F} \boldsymbol{S} \boldsymbol{F}^T : \frac{1}{2} \left( \boldsymbol{F}^T \right)^{-1} \left( D_{\boldsymbol{\chi}} \boldsymbol{C} \cdot \boldsymbol{v} \right) \boldsymbol{F}^{-1} \, d\Omega_R = \int_{\Sigma} \boldsymbol{t} \cdot \boldsymbol{v} \, d\Sigma - \int_{\Omega} \rho \ddot{\boldsymbol{U}} \cdot \boldsymbol{v} \, d\Omega,$$

$$\int_{\Omega_R} \frac{1}{2} \boldsymbol{S} : \left( D_{\boldsymbol{\chi}} \boldsymbol{C} \cdot \boldsymbol{v} \right) d\Omega_R = \int_{\Sigma} \boldsymbol{t} \cdot \boldsymbol{v} \, d\Sigma - \int_{\Omega} \rho \ddot{\boldsymbol{U}} \cdot \boldsymbol{v} \, d\Omega. \tag{3.2}$$

For hyperelastic materials there is a stored energy function $W(\boldsymbol{X}, \boldsymbol{C}(\boldsymbol{\chi}))$ such that the second Piola-Kirchhoff stress tensor can be determined from $W$ through the equation (2.11). Using (2.17) in (3.2) yields

$$\int_{\Omega_R} \frac{\partial W}{\partial \boldsymbol{C}} : D_{\boldsymbol{\chi}} \boldsymbol{C} \cdot \boldsymbol{v} \, d\Omega_R = \int_{\Sigma} \boldsymbol{t} \cdot \boldsymbol{v} \, d\Sigma - \int_{\Omega} \rho \ddot{\boldsymbol{U}} \cdot \boldsymbol{v} \, d\Omega,$$

$$D_{\boldsymbol{\chi}} \left( \int_{\Omega_R} W \, d\Omega_R \right) \cdot \boldsymbol{v} - \int_{\Sigma} \boldsymbol{t} \cdot \boldsymbol{v} \, d\Sigma - \int_{\Omega} \rho \ddot{\boldsymbol{U}} \cdot \boldsymbol{v} \, d\Omega = 0. \tag{3.3}$$

The equation (3.3) represents the *principle of virtual work* in the case when there is a stored energy function $W$. The equation (3.3) also allows the definition of the following functional

$$\mathcal{L}(\boldsymbol{\chi}) = \int_{\Omega_R} W \, d\Omega_R - \int_{\Sigma} \boldsymbol{t} \boldsymbol{\chi} \, d\Sigma + \int_{\Omega} \rho \ddot{\boldsymbol{U}} \boldsymbol{\chi} \, d\Omega. \tag{3.4}$$

The functional (3.4) can be used to derive the weak form and further the finite element equations of the problem for compressible materials. The difficulty arises when the material tends to be incompressible, as in the case of plasticity problems or in the problems involving rubber or rubber-like materials. In this case, in the finite element modeling, it is known that the displacement and the pressure $P$ ($= \sigma_{kk} = \operatorname{tr}\boldsymbol{\sigma}$) are decoupled and therefore separate modeling is needed for each. This formulation is known as *displacement/pressure* formulation [51][12]. A situation which might occur in this case is the *locking* phenomenon caused by the dependency of displacements and pressure determination of the bulk modulus. The fact that an element will lock or not is determined by the Babuska-Brezzi condition [12][13]. The evaluation of this condition is not very easy, and therefore, in practice, this verification is avoided. It is used instead a constrain counts indicator [13].

The incompressibility condition acts like an internal constraint and in the numerical calculus cannot be imposed unless it is introduced explicitly. In the finite element formulation, this can be achieved through the Lagrange multiplier method, penalty method, or the augmented Lagrangian method [12][42]. This leads to an additional variable in the functional (3.4). Using the Lagrange multiplier method and the constraint condition $J = \det[\boldsymbol{C}] = 1$, the functional (3.4) needs to be modified as follows

$$\mathcal{L}(\boldsymbol{\chi}) = \int_{\Omega_R} W \, d\Omega_R + \int_{\Omega_R} P(J-1) \, d\Omega_R - \int_{\Sigma} \boldsymbol{t}\boldsymbol{\chi} \, d\Sigma + \int_{\Omega} \rho \ddot{\boldsymbol{U}} \boldsymbol{\chi} \, d\Omega. \tag{3.5}$$

The functional (3.4) defines the balance of energy. To maintain the same physical meaning of (3.5), the term $P(J-1)$ must have an *energy* dimension. $J-1$ defines in fact the change in the volume or the relative volume of an infinitesimal material element and therefore a *volumetric* deformation. It follows that $P$, the Lagrange multiplier, must have the dimension of a *stress*. The condition $P(J-1) = 0$ states in fact that the mechanical work done by the $P$ over the volumetric deformation is null. The weak form of this condition is the integral form. Different other formulations can be followed in [12] and [51]. The condition $J = 1$ is the particular case of $J = \Theta$ with $\Theta > 0$, $\Theta \to 1$. Using the deformation decomposition (2.34),

it can be written

$$\boldsymbol{F} = J^{1/3}\tilde{\boldsymbol{F}} = \Theta^{1/3}\Theta^{-1/3}J^{1/3}\tilde{\boldsymbol{F}}.$$

This suggests the consideration of a modified deformation gradient $\overline{\boldsymbol{F}}$ instead of $\boldsymbol{F}$

$$\overline{\boldsymbol{F}}(\boldsymbol{\chi},\Theta) = \Theta^{1/3}\tilde{\boldsymbol{F}}(\boldsymbol{\chi}) = \Theta^{1/3}J(\boldsymbol{\chi})^{-1/3}\boldsymbol{F}, \quad \overline{\boldsymbol{C}} = \overline{\boldsymbol{F}}^T\overline{\boldsymbol{F}}, \quad J(\boldsymbol{\chi}) = \det \boldsymbol{F}, \tag{3.6}$$

where $\overline{\boldsymbol{C}}$ is the associated right Cauchy-Green tensor with the modified deformation gradient. It is clear that if we impose now the condition $J(\boldsymbol{\chi}) = \Theta$, it follows that $\overline{\boldsymbol{F}} = \boldsymbol{F}$. This moves the incompressibility condition $\Theta \to 1$ to be imposed on $W$. Hence the functional (3.5) can be modified by replacing $\boldsymbol{F}$ with $\overline{\boldsymbol{F}}$ and 1 with $\Theta$. This leads to the following functional depending on three fields $(\boldsymbol{\chi}, P, \Theta)$

$$\mathcal{L}(\boldsymbol{\chi},\Theta,P) = \int_{\Omega_R}\left[W\left(\boldsymbol{X},\overline{\boldsymbol{C}}(\boldsymbol{\chi},\Theta)\right) + P(J(\boldsymbol{\chi})-\Theta)\right]d\Omega_R - \int_\Sigma \boldsymbol{t}\boldsymbol{\chi}\,d\Sigma + \int_\Omega \rho\ddot{\boldsymbol{U}}\boldsymbol{\chi}\,d\Omega. \tag{3.7}$$

It can be seen that (3.7) does not impose any restriction yet on $W$ regarding the incompressibility condition. This condition can be added later by a proper choice of the stored energy function. So far the functional (3.7) holds for both types of materials: compressible as well as incompressible. The extended virtual work principle (3.3) in the case of (3.7) is

$$D_{\boldsymbol{\chi}}\mathcal{L}\cdot\boldsymbol{v} + D_\Theta\mathcal{L}\cdot\vartheta + D_P\mathcal{L}\cdot q = 0, \tag{3.8}$$

where $\vartheta$ and $q$ are admissible variations of $\Theta$ respectively $P$. The equation (3.8) yields to the following three equations

$$\int_{\Omega_R}\left(D_{\boldsymbol{\chi}}W\cdot\boldsymbol{v} + PD_{\boldsymbol{\chi}}J(\boldsymbol{\chi})\cdot\boldsymbol{v}\right)d\Omega_R = \int_\Sigma \boldsymbol{t}\cdot\boldsymbol{v}\,d\Sigma - \int_\Omega \rho\ddot{\boldsymbol{U}}\cdot\boldsymbol{v}\,d\Omega, \tag{3.9}$$

$$\int_{\Omega_R}\left(D_\Theta W\cdot\vartheta - P\vartheta\right)d\Omega_R = 0, \tag{3.10}$$

$$\int_{\Omega_R} q\left(J(\boldsymbol{\chi})-\Theta\right)d\Omega_R = 0. \tag{3.11}$$

Using the results from the section 3.6, we obtain

$$\int_\Omega \left\{ \mathrm{dev}\left[ \frac{2}{J}\overline{\boldsymbol{F}}\,\frac{\partial W}{\partial \overline{\boldsymbol{C}}}\,\overline{\boldsymbol{C}}\,\overline{\boldsymbol{F}}^T \right] : \mathrm{dev}\left[\bigtriangledown \boldsymbol{v}\right] + P\,\mathrm{div}\,\boldsymbol{v} \right\} d\Omega = \int_\Sigma \boldsymbol{t}\cdot\boldsymbol{v}\,d\Sigma - \int_\Omega \rho\ddot{\boldsymbol{U}}\cdot\boldsymbol{v}\,d\Omega, \quad (3.12)$$

$$\int_\Omega \vartheta \left[ \frac{J}{3\Theta}\mathrm{tr}\left( \frac{2}{J}\overline{\boldsymbol{F}}\,\frac{\partial W}{\partial \overline{\boldsymbol{C}}}\,\overline{\boldsymbol{F}}^T \right) - P \right\} \frac{1}{J}\,d\Omega = 0, \quad (3.13)$$

$$\int_\Omega q\,(J(\boldsymbol{\chi}) - \Theta)\,\frac{1}{J}\,d\Omega = 0, \quad (3.14)$$

or in a different form

$$\int_\Omega \left\{ \mathrm{dev}\,\boldsymbol{\sigma} : \mathrm{dev}\left[\bigtriangledown \boldsymbol{v}\right] + P\,\mathrm{div}\,\boldsymbol{v} \right\} d\Omega = \int_\Sigma \boldsymbol{t}\cdot\boldsymbol{v}\,d\Sigma - \int_\Omega \rho\,\ddot{\boldsymbol{U}}\cdot\boldsymbol{v}\,d\Omega, \quad (3.15)$$

$$\int_\Omega \vartheta \left[ \frac{J}{3\Theta}\mathrm{tr}\,\boldsymbol{\sigma} - P \right\} \frac{1}{J}\,d\Omega = 0, \quad (3.16)$$

$$\int_\Omega q\,(J - \Theta)\,\frac{1}{J}\,d\Omega = 0. \quad (3.17)$$

The equations (3.12)-(3.17) are the weak form of the equations (2.23) or (2.24) and are valid for any expression of the stored energy function $W$. Using the decomposition (2.35) the stored energy function can be written

$$W\left(\boldsymbol{X}, \overline{\boldsymbol{C}}(\boldsymbol{\chi}, \Theta)\right) = U(\Theta) + \tilde{W}\left(\boldsymbol{X}, \tilde{\boldsymbol{C}}\right), \quad (3.18)$$

in which the first part $U(\Theta)$ is the energy stored as a volumetric deformation and $\tilde{W}\left(\boldsymbol{X}, \tilde{\boldsymbol{C}}\right)$ the energy stored as a deviatoric deformation. From the equation (3.17) it follows that $\Theta = J$. Introducing this result in (3.16) yields

$$P = \frac{1}{3}\mathrm{tr}\,\boldsymbol{\sigma} = \frac{1}{3}\sigma_{kk} = U^{'}(J). \quad (3.19)$$

From the equation (3.19) it can be seen that the Lagrange multiplier $P$ is like *a pressure*, but it is not *the pressure* as in fluid mechanics, for example. Using (3.19), the second Piola-Kirchhoff stress tensor becomes

$$\boldsymbol{S} = 2\frac{\partial W}{\partial \boldsymbol{C}} = 2\frac{\partial U}{\partial J}\frac{\partial J}{\partial \boldsymbol{C}} + 2\frac{\partial \tilde{W}}{\partial \boldsymbol{C}} = U^{'}J\boldsymbol{C}^{-1} + 2\frac{\partial \tilde{W}}{\partial \boldsymbol{C}}.$$

Using the derivations formulae from section 3.6 we obtain

$$\boldsymbol{S} = PJ\boldsymbol{C}^{-1} + 2J^{-2/3}\mathrm{DEV}\left(\frac{\partial \tilde{W}}{\partial \tilde{\boldsymbol{C}}}\right), \quad \mathrm{DEV}[\cdot] = [\cdot] - \frac{1}{3}\left([\cdot] : \boldsymbol{C}\right)\boldsymbol{C}^{-1}, \tag{3.20}$$

$$\boldsymbol{\sigma} = P\mathbf{1} + \frac{2}{J}\mathrm{dev}\left(\tilde{\boldsymbol{F}}\frac{\partial \tilde{W}}{\partial \tilde{\boldsymbol{C}}}\tilde{\boldsymbol{F}}^{T}\right). \tag{3.21}$$

### 3.1.1 Incompressibility condition

With the previous weak formulation, the incompressibility condition $\Theta = 1$ can be introduced by a proper choice of the function $U(\Theta)$. However the function $U(\Theta)$ must satisfy two conditions.

- $U(\Theta) \geq 0$ and convex. This condition is imposed by the fact that the energy must be positive or zero and must remain a convex function.
- $U(\Theta) = 0 \equiv \Theta = 1$. This condition is required by the incompressibility condition.

Analyzing the expression (2.32), it is suggested to consider for the volumetric part of $W$

$$U(\Theta) = Kf(\Theta), \qquad K = \frac{2G(1+\nu)}{3(1-2\nu)},$$

where $K$ represents the bulk modulus, and the condition for $U(\Theta)$ is now transferred to $f(\Theta)$. As long as the above requirements are satisfied, any function $f(\Theta)$ can be chosen. In the case of rubber material $\nu \to 0.5 \Rightarrow K \to \infty$ and $K$ acts like a penalty parameter for a constraint condition $f(\Theta) = 0$ which, is equivalent to $\Theta \to 1$. So, in fact, by choosing $f(\Theta)$ satisfying the above requirements and choosing $\nu \approx 0.5$, we impose the constraint condition $\Theta = 1$. For example in [49]

$$f(\Theta) = \frac{1}{2}\left[(x^2 - 1) - \ln\Theta\right],$$

is used for rubber-like materials analysis. In [49]

$$f(\Theta) = K\left[\ln\Theta\right]^2, \tag{3.22}$$

is used in the elasto-plastic analysis. The finite element program NIKE3D uses the function (3.22) for a Mooney-Rivlin model, see also section 2.5. The penalty method exposed here can be further improved by using the augmented Lagrangian method [50].

## 3.2 Linearization. Static case

The equations (2.23),(2.24), the strong form, or (3.12)-(3.17), the weak form, are nonlinear equations. The usual procedure for solving those equations is an iterative method, which requires a linearization of those equations. In Chapter 2, the linearized equations of the strong form was presented. In this section the liniarization of the weak form is presented, an essential step for solving the problem using the Finite Element Method. To proceed, first we write the equations (3.12)-(3.14) in the reference configuration. Introducing (2.14) and the results from section 3.6, we obtain

$$\int_{\Omega_R} \overline{\boldsymbol{F}}\,\overline{\boldsymbol{S}} : \mathrm{GRAD}\,\boldsymbol{v}\, d\Omega_R = \int_{\Sigma} \boldsymbol{t}\cdot\boldsymbol{v}\, d\Sigma, \tag{3.23}$$

$$\int_{\Omega_R} \vartheta \left(U'(\Theta) - P\right) d\Omega_R = 0, \tag{3.24}$$

$$\int_{\Omega_R} q(J-\Theta)\, d\Omega_R = 0. \tag{3.25}$$

Following the definition of the linearization process, we consider small increments $(\boldsymbol{u},\theta,p)$ of $(\boldsymbol{U},\Theta,P)$. The Gateaux derivative in the direction $(\boldsymbol{u},\theta,p)$ of the equation (3.23) yields

$$D_{\boldsymbol{u}}\left\{\int_{\Omega_R} \overline{\boldsymbol{F}}\,\overline{\boldsymbol{S}} : \mathrm{GRAD}\,\boldsymbol{v}\, d\Omega_R\right\}\cdot\boldsymbol{u} + D_p\left\{\int_{\Omega_R} \overline{\boldsymbol{F}}\,\overline{\boldsymbol{S}} : \mathrm{GRAD}\,\boldsymbol{v}\, d\Omega_R\right\}\cdot p =$$

$$= \int_{\Sigma} \boldsymbol{t}\cdot\boldsymbol{v}\, d\Sigma - \int_{\Omega} \bigtriangledown\boldsymbol{v} : \boldsymbol{\sigma}\, d\Omega \tag{3.26}$$

The left hand side of the equation (3.26) can be expanded as follows

$$D_{\boldsymbol{u}}\Big\{\int_{\Omega_R} \overline{\boldsymbol{F}}\,\overline{\boldsymbol{S}} : \mathrm{GRAD}\,\boldsymbol{v}\,d\Omega_R\Big\}\cdot\boldsymbol{u} + D_p\Big\{\int_{\Omega_R} \overline{\boldsymbol{F}}\,\overline{\boldsymbol{S}} : \mathrm{GRAD}\,\boldsymbol{v}\,d\Omega_R\Big\}\cdot p =$$

$$= \int_{\Omega_R}\left[\left(D_{\boldsymbol{u}}\overline{\boldsymbol{F}}\cdot\boldsymbol{u}\right)\overline{\boldsymbol{S}} + \overline{\boldsymbol{F}}\left(D_{\boldsymbol{u}}\overline{\boldsymbol{S}}\cdot\boldsymbol{u}\right)\right] : \mathrm{GRAD}\,\boldsymbol{v}\,d\Omega_R + D_p\Big\{\int_{\Omega_R} \overline{\boldsymbol{F}}\,\overline{\boldsymbol{S}} : \mathrm{GRAD}\,\boldsymbol{v}\,d\Omega_R\Big\}\cdot p. \tag{3.27}$$

Using the formulae from section 3.6 in (3.27) yields

$$\int_{\Omega_R} \bigtriangledown\boldsymbol{u}\overline{\boldsymbol{F}}\,\overline{\boldsymbol{S}} : \mathrm{GRAD}\boldsymbol{v}\,d\Omega_R +$$

$$+\int_{\Omega_R}\left(\overline{\boldsymbol{F}}\left\{J\overline{\boldsymbol{F}}^{-1}\left[P\left(\mathbf{1}\otimes\mathbf{1}-2\mathbf{I}\right)\right]\left(\overline{\boldsymbol{F}}^{T}\right)^{-1} + \overline{\boldsymbol{F}}\tilde{\mathbf{C}}\overline{\boldsymbol{F}}^{T}\right\} : \bigtriangledown^{s}\boldsymbol{u} + p\mathbf{1}\right) : \mathrm{GRAD}\,\boldsymbol{v}\,d\Omega_R.$$

in the reference configuration. In the present configuration (3.27) becomes

$$\int_{\Omega} \bigtriangledown\boldsymbol{v} : \left\{(\bigtriangledown\boldsymbol{u})\boldsymbol{\sigma} + \left[P\left(\mathbf{1}\otimes\mathbf{1}-2\mathbf{I}\right) + \tilde{\mathbf{c}}\right] : \bigtriangledown\boldsymbol{u} + p\mathbf{1}\right\} d\Omega$$

where $\tilde{\mathbf{C}}$ and $\tilde{\mathbf{c}}$ are the *deviatoric* material tensors expressed in reference and present configuration [50].

$$\left(\mathbf{1}\otimes\mathbf{1}\right)_{ijkl} = \delta_{ij}\delta_{kl}, \qquad \left(\mathbf{I}\right)_{ijkl} = \delta_{ik}\delta_{jl}$$

Following the definition (2.20) and the decoupled form (2.35) of stored energy function we obtain

$$\mathbf{C} = 4\frac{\partial W}{\partial\boldsymbol{C}\partial\boldsymbol{C}} = 2\frac{\partial\boldsymbol{S}}{\partial\boldsymbol{C}} = 2\frac{\partial}{\partial\boldsymbol{C}}\left\{PJ\boldsymbol{C}^{-1} + 2J^{-2/3}\left[\frac{\partial\tilde{W}}{\partial\boldsymbol{C}} - \frac{1}{3}\left(\frac{\partial\tilde{W}}{\partial\boldsymbol{C}} : \boldsymbol{C}\right)\boldsymbol{C}^{-1}\right]\right\}.$$

A complete derivation of $\mathbf{C}$ and $\mathbf{c}$ can be found in [56]. Hence the linearized form of the weak form (3.23) in the present configuration is

$$\int_{\Omega} \bigtriangledown^{s}\boldsymbol{v} : \left\{(\bigtriangledown^{s}\boldsymbol{u})\boldsymbol{\sigma} + \left[P\left(\mathbf{1}\otimes\mathbf{1}-2\mathbf{I}\right) + \tilde{\mathbf{c}}\right] : \bigtriangledown^{s}\boldsymbol{u} + p\mathbf{1}\right\} d\Omega =$$

$$= \int_{\Sigma} \boldsymbol{v}\cdot\boldsymbol{t}\,d\Sigma - \int_{\Omega} \bigtriangledown\boldsymbol{v} : \boldsymbol{\sigma}\,d\Omega. \tag{3.28}$$

Similarly the linearized form of (3.24) is

$$\int_{\Omega} \vartheta \left( U^{''}(\Theta)\theta - p \right) d\Omega = - \int_{\Omega} \vartheta \left( U^{'}(\Theta) - P \right) d\Omega, \tag{3.29}$$

and for the third equation (3.25)

$$\int_{\Omega} q(\operatorname{div} \boldsymbol{u} - \frac{1}{J}\theta)\, d\Omega = - \int_{\Omega} q(J - \Theta)\, d\Omega. \tag{3.30}$$

For the finite element formulation it is convenient that (3.28), (3.29) and (3.30) be written in matrix form. Similar with [46], we introduce the following notations

$$\boldsymbol{\mathcal{B}}_{L} = \begin{bmatrix} \frac{\partial}{\partial x_1} & 0 & 0 \\ 0 & \frac{\partial}{\partial x_2} & 0 \\ 0 & 0 & \frac{\partial}{\partial x_3} \\ \frac{\partial}{\partial x_1} & \frac{\partial}{\partial x_2} & 0 \\ \frac{\partial}{\partial x_1} & 0 & \frac{\partial}{\partial x_3} \\ 0 & \frac{\partial}{\partial x_2} & \frac{\partial}{\partial x_3} \end{bmatrix}, \quad \boldsymbol{\mathcal{B}}_{NL} = \begin{bmatrix} \frac{\partial}{\partial x_1} & 0 & 0 \\ 0 & \frac{\partial}{\partial x_1} & 0 \\ 0 & 0 & \frac{\partial}{\partial x_1} \\ \frac{\partial}{\partial x_2} & 0 & 0 \\ 0 & \frac{\partial}{\partial x_2} & 0 \\ 0 & 0 & \frac{\partial}{\partial x_2} \\ \frac{\partial}{\partial x_3} & 0 & 0 \\ 0 & \frac{\partial}{\partial x_3} & 0 \\ 0 & 0 & \frac{\partial}{\partial x_3} \end{bmatrix}, \quad \boldsymbol{\mathcal{D}} = \begin{bmatrix} \frac{\partial}{\partial x_1} \\ \frac{\partial}{\partial x_2} \\ \frac{\partial}{\partial x_3} \end{bmatrix},$$

$$\mathbf{S} = \begin{bmatrix} \boldsymbol{\sigma}_{11} & \boldsymbol{\sigma}_{12} & \boldsymbol{\sigma}_{13} \\ \boldsymbol{\sigma}_{21} & \boldsymbol{\sigma}_{22} & \boldsymbol{\sigma}_{23} \\ \boldsymbol{\sigma}_{31} & \boldsymbol{\sigma}_{32} & \boldsymbol{\sigma}_{33} \end{bmatrix}, \qquad \boldsymbol{\sigma}_{ij} = \begin{bmatrix} \sigma_{ij} & 0 & 0 \\ 0 & \sigma_{ij} & 0 \\ 0 & 0 & \sigma_{ij} \end{bmatrix},$$

$$\boldsymbol{\sigma}^{T} = \begin{bmatrix} \sigma_{11} & \sigma_{22} & \sigma_{33} & \sigma_{12} & \sigma_{13} & \sigma_{23} \end{bmatrix}, \quad \boldsymbol{u} = \begin{Bmatrix} u_1 \\ u_2 \\ u_3 \end{Bmatrix}, \quad \boldsymbol{v} = \begin{Bmatrix} v_1 \\ v_2 \\ v_3 \end{Bmatrix}.$$

The components of the second order symmetric gradient tensor $\bigtriangledown^{s}\boldsymbol{u}$ can be arranged in a vector

$$\boldsymbol{e}^{T} = \begin{bmatrix} e_{11} & e_{22} & e_{33} & 2e_{12} & 2e_{13} & 2e_{23} \end{bmatrix}, \quad e_{ij} = \frac{1}{2}\left(u_{i,j} + u_{j,i}\right), \quad \boldsymbol{e} = \boldsymbol{\mathcal{B}}_{L}\boldsymbol{u},$$

and the components of the forth order material tensor $\mathbf{C}$ in a $6 \times 6$ matrix

$$\mathbf{C} = \begin{bmatrix} \mathrm{C}_{1111} & \mathrm{C}_{1122} & \mathrm{C}_{1133} & \mathrm{C}_{1112} & \mathrm{C}_{1113} & \mathrm{C}_{1123} \\ \mathrm{C}_{2211} & \mathrm{C}_{2222} & \mathrm{C}_{2233} & \mathrm{C}_{2212} & \mathrm{C}_{2213} & \mathrm{C}_{2223} \\ \mathrm{C}_{3311} & \mathrm{C}_{3322} & \mathrm{C}_{3333} & \mathrm{C}_{3312} & \mathrm{C}_{3313} & \mathrm{C}_{3323} \\ \mathrm{C}_{1211} & \mathrm{C}_{1222} & \mathrm{C}_{1233} & \mathrm{C}_{1212} & \mathrm{C}_{1213} & \mathrm{C}_{1223} \\ \mathrm{C}_{1311} & \mathrm{C}_{1322} & \mathrm{C}_{1333} & \mathrm{C}_{1312} & \mathrm{C}_{1313} & \mathrm{C}_{1323} \\ \mathrm{C}_{2311} & \mathrm{C}_{2322} & \mathrm{C}_{2333} & \mathrm{C}_{2312} & \mathrm{C}_{2313} & \mathrm{C}_{2323} \end{bmatrix}.$$

The equation (3.28) can be written

$$\int_\Omega \boldsymbol{v}^T \boldsymbol{\mathcal{B}}_L^T \mathbf{C} \boldsymbol{\mathcal{B}}_L \boldsymbol{u} \, d\Omega + \int_\Omega \boldsymbol{v}^T \boldsymbol{\mathcal{B}}_{NL}^T \boldsymbol{S} \boldsymbol{\mathcal{B}}_{NL} \, d\Omega + \int_\Omega p \boldsymbol{\mathcal{D}}^T \boldsymbol{v} \, d\Omega =$$

$$= \int_\Sigma \boldsymbol{v}^T \boldsymbol{t} \, d\Sigma - \int_\Omega \boldsymbol{v}^T \boldsymbol{\mathcal{B}}_L^T \boldsymbol{\sigma} \, d\Omega. \tag{3.31}$$

The second equation (3.29) remains the same

$$\int_\Omega \vartheta \left( U^{''}(\Theta)\theta - p \right) d\Omega = - \int_\Omega \vartheta \left( U^{'}(\Theta) - P \right) d\Omega, \tag{3.32}$$

and the third equation

$$\int_\Omega q(\boldsymbol{\mathcal{D}}^T \boldsymbol{u} - \frac{1}{J}\theta) \, d\Omega = - \int_\Omega q(J - \Theta) \, d\Omega. \tag{3.33}$$

## 3.3 Finite element equation. Static case

Let $\Omega = \cup \Omega_e$ be a discretization of the domain $\Omega$ in the present configuration. On each element $\Omega_e$ we introduce a continuum approximation of the displacement $\boldsymbol{u}$ using the standard shape functions and nodal values [12][58].

$$\boldsymbol{u} = \boldsymbol{\Phi}^T \mathbf{u}, \qquad \mathbf{u}^T = \left[ \boldsymbol{u}^1 \ \boldsymbol{u}^2 \ \ldots \ \boldsymbol{u}^n \right], \tag{3.34}$$

and a discontinuous approximation of the relative volume $\theta$ and the pressure $p$ using standard shape functions, but internal values.

$$\theta = \boldsymbol{\Psi}^T \boldsymbol{\theta}, \qquad p = \boldsymbol{\Psi}^T \mathbf{p}. \tag{3.35}$$

Similarly the variables $(\boldsymbol{\upsilon}, \vartheta, q)$ will be replaced by

$$\boldsymbol{\upsilon} \longrightarrow \boldsymbol{\Phi}^T \boldsymbol{\upsilon}, \quad \boldsymbol{\upsilon}^T = \left[\boldsymbol{\upsilon}^1 \ \boldsymbol{\upsilon}^2 \ \ldots \ \boldsymbol{\upsilon}^n\right], \quad \vartheta \longrightarrow \boldsymbol{\Psi}^T \boldsymbol{\vartheta}, \quad q \longrightarrow \boldsymbol{\Psi}^T \boldsymbol{q}.$$

Introducing the matrices

$$\mathbf{B}_L = \boldsymbol{\mathcal{B}}_L \boldsymbol{\Phi}, \quad \mathbf{B}_{NL} = \boldsymbol{\mathcal{B}}_{NL} \boldsymbol{\Phi}, \quad \mathbf{D} = \boldsymbol{\mathcal{D}} \boldsymbol{\Phi},$$

the linearized equation (3.28) becomes

$$\boldsymbol{\upsilon}^T \int_{\Omega_e} \mathbf{B}_L^T \mathbf{C} \mathbf{B}_L \, d\Omega \ \mathbf{u} + \boldsymbol{\upsilon}^T \int_{\Omega_e} \mathbf{B}_{NL}^T \boldsymbol{S} \mathbf{B}_{NL} \, d\Omega \ \mathbf{u} + \boldsymbol{q}^T \int_{\Omega_e} \mathbf{D} \boldsymbol{\Psi}^T \, d\Omega \ \mathbf{p} =$$

$$= \boldsymbol{\upsilon}^T \int_{\Sigma} \boldsymbol{\Phi}^T \boldsymbol{t} \, d\Sigma - \boldsymbol{\upsilon}^T \int_{\Omega_e} \mathbf{B}_L^T \boldsymbol{\sigma} \, d\Omega,$$

The second equation

$$\boldsymbol{\vartheta}^T \int_{\Omega_e} U''(\Theta) \boldsymbol{\Psi} \boldsymbol{\Psi}^T \, d\Omega \ \boldsymbol{\theta} - \boldsymbol{\vartheta}^T \int_{\Omega_e} \boldsymbol{\Psi} \boldsymbol{\Psi}^T \, d\Omega \, \mathbf{p} = -\boldsymbol{\vartheta}^T \int_{\Omega_e} \boldsymbol{\Psi} \left[U'(\Theta) - p\right] \, d\Omega,$$

and the third equation

$$\boldsymbol{q}^T \int_{\Omega_e} \boldsymbol{\Psi} \mathbf{D}^T \, d\Omega \, \mathbf{u} - \boldsymbol{q}^T \int_{\Omega_e} \frac{1}{J} \boldsymbol{\Psi} \boldsymbol{\Psi}^T \, d\Omega \, \boldsymbol{\theta} = -\boldsymbol{q}^T \int_{\Omega_e} \boldsymbol{\Psi} \left(J - \Theta\right) \, d\Omega.$$

Since the variations $\boldsymbol{\upsilon}, \boldsymbol{\vartheta}, \boldsymbol{q}$ are arbitrary, it follows that

$$\begin{bmatrix} \mathbf{K}_{uu} & 0 & \mathbf{K}_{up} \\ 0 & \mathbf{K}_{\theta\theta} & \mathbf{K}_{\theta p} \\ \mathbf{K}_{pu} & \mathbf{K}_{p\theta} & 0 \end{bmatrix} \begin{Bmatrix} \mathbf{u} \\ \boldsymbol{\theta} \\ \mathbf{p} \end{Bmatrix} = \begin{Bmatrix} \mathbf{F}_u \\ \mathbf{F}_\theta \\ \mathbf{F}_p \end{Bmatrix}. \tag{3.36}$$

The equation (3.36) represents the finite element equation. The matrices in (3.36) are defined as follows

$$\mathbf{K}_{uu} = \int_{\Omega_e} \mathbf{B}_L^T \mathbf{C} \mathbf{B}_L \, d\Omega + \int_{\Omega_e} \mathbf{B}_{NL}^T \boldsymbol{S} \mathbf{B}_{NL} \, d\Omega, \tag{3.37}$$

$$\mathbf{K}_{up} = \int_{\Omega_e} \mathbf{D} \boldsymbol{\Psi}^T \, d\Omega, \qquad \mathbf{K}_{\theta p} = \int_{\Omega_e} \boldsymbol{\Psi} \boldsymbol{\Psi}^T \, d\Omega,$$

$$\mathbf{K}_{\theta\theta} = \int_{\Omega_e} U^{''}(\theta)\boldsymbol{\Psi}\boldsymbol{\Psi}^T \, d\Omega, \qquad \mathbf{K}_{pu} = \int_{\Omega_e} \boldsymbol{\Psi}\mathbf{D}^T \, d\Omega,$$

$$\mathbf{K}_{p\theta} = \int_{\Omega_e} \frac{1}{J}\boldsymbol{\Psi}\boldsymbol{\Psi}^T \, d\Omega.$$

The matrix $\mathbf{K}_{uu}$ is the displacement tangent stiffness matrix of the element $e$. The first term in (3.37) represents the material stiffness matrix, and the second term the geometric or initial stress stiffness matrix. The vectors on the right side of the equation (3.36) are defined below

$$\mathbf{F}_u = \int_{\Sigma} \boldsymbol{\Phi}^T \boldsymbol{t} \, d\Sigma - \int_{\Omega} \mathbf{B}_L^T \boldsymbol{\sigma} \, d\Omega = \mathbf{F}^{ext} - \mathbf{F}^{int}(\mathbf{U}), \tag{3.38}$$

$$\mathbf{F}_\Theta = \int_{\Omega_e} \boldsymbol{\Psi} \left[ U^{'}(\Theta) - p \right] \, d\Omega,$$

$$\mathbf{F}_p = \int_{\Omega_e} \boldsymbol{\Psi} \left( J - \Theta. \right) \, d\Omega$$

The first term in (3.38) represents the force due to the external loads and the second term the internal force. The equation (3.36) can be assembled in full size, keeping all variables. But due to the structure of the equation (3.36)the variables $\boldsymbol{\theta}$ and $\mathbf{p}$ can be condensed at the element level. We present below two methods.

### 3.3.1 Static condensation-I

From the second equation of (3.36)

$$\boldsymbol{\theta} = \mathbf{K}_{\theta\theta}^{-1} \left( \mathbf{F}_\theta - \mathbf{K}_{\theta\theta}\mathbf{p} \right), \tag{3.39}$$

and from the third equation of (3.36) $\mathbf{p}$ can be expressed

$$\mathbf{p} = \mathbf{G}\mathbf{u} + \mathbf{h}, \tag{3.40}$$

where

$$\mathbf{G} = \left(\mathbf{K}_{p\theta}\mathbf{K}_{\theta\theta}^{-1}\mathbf{K}_{\theta p}\right)^{-1}\mathbf{K}_{pu}, \qquad \mathbf{h} = \left(\mathbf{K}_{p\theta}\mathbf{K}_{\theta\theta}^{-1}\mathbf{K}_{\theta p}\right)^{-1}\left(\mathbf{K}_{p\theta}\mathbf{K}_{\theta\theta}^{-1}\mathbf{F}_{\theta} - \mathbf{F}_{p}\right).$$

Substituting (3.40) in the first equation of (3.36) yields

$$\mathbf{K}_T^e\left(\mathbf{U}_e\right)\mathbf{u}_e = \mathbf{F}^e\left(\mathbf{U}_e\right), \tag{3.41}$$

where $e$ indicates that the equation (3.41) refers to the element $e$ and

$$\mathbf{K}_T^e = \mathbf{K}_{uu}^e + \mathbf{K}_{up}^e\mathbf{G}^e, \qquad \mathbf{F}^e = \mathbf{F}_u^e + \mathbf{K}_{up}^e\mathbf{h}^e.$$

Assembling all equations (3.41) for all elements yields

$$\mathbf{K}_T\left(\mathbf{U}\right)\mathbf{u} = \mathbf{F}\left(\mathbf{U}\right), \tag{3.42}$$

where $\mathbf{K}_T(\mathbf{u})$ represents the tangent matrix of the finite element model, $\mathbf{u}$ the vector of the increment displacements, which needs to be determined, and $\mathbf{F}(\mathbf{u})$ the force vector. The equation (3.42) is a nonlinear equation and can be solved iteratively by different methods [12]. One of these methods is described in section 3.5.1. After solving (3.42) for displacements, then $\boldsymbol{\theta}$ and $\mathbf{p}$ are calculated using (3.39), (3.40) and (3.34) respectively. The values of displacement, relative volume and pressure are updated using

$$\mathbf{U} \longrightarrow \mathbf{U} + \mathbf{u}, \qquad \Theta \longrightarrow \Theta + \theta, \qquad P \longrightarrow P + p.$$

### 3.3.2 Static condensation-II

In section 3.3 we have solved the problem using a finite element approximation (3.35) for the *increments* of pressure $\mathbf{p}$ and relative volume $\boldsymbol{\theta}$. In the end, the pressure and the relative volume were statically condensed at the element level resulting finally in a nonlinear equation only in $\mathbf{u}$. This suggests that the way in which the pressure and the relative volume are calculated at the element level does not affect the final equation, which will be only a function of $\mathbf{u}$.

Using this idea Simo and Taylor proposed a different approach in [50] for calculating the *total pressure* $P$ and the *total relative volume* $\Theta$. In this approach the *total pressure* and *total relative volume* are approximated at the element level using again shape functions and internal values of the *total pressure* and *total relative volume*.

$$\Theta = \mathbf{\Psi}^T \mathbf{\Theta}, \qquad P = \mathbf{\Psi}^T \mathbf{P}, \tag{3.43}$$

where this time the vector $\mathbf{P}$ and $\mathbf{\Theta}$ contains the values of total relative volume and total pressure on an element. Replacing (3.43) in the equation (3.16) and (3.17), we obtain

$$\mathbf{\Theta}^T \int_{\Omega_R} J\mathbf{\Psi}\, d\Omega_R = \mathbf{\Theta}^T \int_{\Omega_R} \mathbf{\Psi}\mathbf{\Psi}^T\, d\Omega_R\, \mathbf{\Theta},$$

and further

$$\mathbf{\Theta} = \mathbf{K}_{\Theta\Theta}^{-1}\mathbf{F}_\Theta, \qquad \mathbf{K}_{\Theta\Theta} = \int_{\Omega_R} \mathbf{\Psi}\mathbf{\Psi}^T\, d\Omega_R, \qquad \mathbf{F}_\Theta = \int_{\Omega_R} J\mathbf{\Psi}\, d\Omega_R. \tag{3.44}$$

Introducing (3.44) in the equation (3.17) yields

$$\mathbf{P}^T \int_{\Omega_R} U^{'}(\Theta)\mathbf{\Psi}\, d\Omega_R = \mathbf{P}^T \int_{\Omega_R} \mathbf{\Psi}\mathbf{\Psi}^T\, d\Omega_R \mathbf{P},$$

and

$$\mathbf{P} = \mathbf{K}_{pp}^{-1}\mathbf{F}_p, \qquad \mathbf{K}_{pp} = \int_{\Omega_R} \mathbf{\Psi}\mathbf{\Psi}^T\, d\Omega_R, \qquad \mathbf{F}_p = \int_{\Omega_R} U^{'}(\Theta)\mathbf{\Psi}\, d\Omega_R. \tag{3.45}$$

The increment $p$ in the linearized equation (3.36) is now calculated from (3.45) and introduced in the first equation of (3.36). The finite element program NIKE3D uses this approach.

## 3.4 Finite element equation. Dynamic case

In the dynamic case the linearization follows the time domain discretization. The usual procedure expreses the displacements at the present time $t + \Delta t$ as a function of the displacements $\boldsymbol{U}$, velocities $\dot{\boldsymbol{U}}$ and accelerations $\ddot{\boldsymbol{U}}$ at the time $t$, leading to a Newmark-$\beta$ time integration schemes [13][32][3]. Following [3] for example,

$${}^{t+\Delta t}\boldsymbol{U} = {}^{t}\boldsymbol{U} + \Delta t\ {}^{t}\dot{\boldsymbol{U}} + \left(\frac{1}{2} - \beta\right)\Delta t^2\ {}^{t}\ddot{\boldsymbol{U}} + \beta\Delta t^2\ {}^{t+\Delta t}\ddot{\boldsymbol{U}}, \tag{3.46}$$

$$ {}^{t+\Delta t}\dot{\boldsymbol{U}} = {}^{t}\dot{\boldsymbol{U}} + (1-\gamma)\,{}^{t}\Delta t\ddot{\boldsymbol{U}} + \gamma\Delta t\,{}^{t+\Delta t}\ddot{\boldsymbol{U}}, \tag{3.47} $$

where $\beta$ and $\gamma$ are numbers between $(0,1)$. Introducing (3.46) in (3.47) and linearizing the equations (3.15)-(3.17) at the time $t+\Delta t$ yields

$$ \mathbf{M}\,{}^{t+\Delta t}\ddot{\mathbf{U}} + \mathbf{K}_T({}^{t}\mathbf{U})\mathbf{u} = {}^{t+\Delta t}\mathbf{F}^{ext} - \mathbf{F}^{int}({}^{t}\mathbf{U}). \tag{3.48} $$

The displacement increment $\mathbf{u}$ can be determined iteratively. At the iteration $k+1$

$$ \mathbf{K}^*({}^{t}\mathbf{U}^k)\,\mathbf{u}^{k+1} = {}^{t+\Delta t}\mathbf{F}^{ext} - \mathbf{F}^*({}^{t+\Delta t}\mathbf{U}^k), \tag{3.49} $$

where

$$ \mathbf{K}^*({}^{t}\mathbf{U}) = \mathbf{K}_T({}^{t}\mathbf{U}^k) + \frac{1}{\beta\Delta t^2}\mathbf{M}, \tag{3.50} $$

$$ \mathbf{F}^*({}^{t+\Delta t}\mathbf{U}^k) = \mathbf{F}^{int}({}^{t}\mathbf{U}^k) + \mathbf{M}\,{}^{t+\Delta t}\ddot{\mathbf{U}}^{k+1}. \tag{3.51} $$

The iterations start with $k=0$ by calculating

$$ \mathbf{K}^* = \mathbf{K}_T({}^{t}\mathbf{U}) + \frac{1}{\beta\Delta t^2}\mathbf{M}, \tag{3.52} $$

with $\mathbf{K}_T({}^{t}\mathbf{U})$ calculated from the last iteration of the previous time step and

$$ \mathbf{F}^* = \mathbf{F}({}^{t}\mathbf{U}) - \mathbf{M}\left[\frac{1}{\beta\Delta t}\,{}^{t}\dot{\mathbf{U}} + \frac{1}{\beta}\left(\frac{1}{2}-\beta\right)\,{}^{t}\ddot{\mathbf{U}}\right]. $$

Solving (3.49) the accelerations, velocities and displacements are updated by

$$ {}^{t+\Delta t}\ddot{\mathbf{U}} = \frac{1}{\beta\Delta t^2}\mathbf{u} - \frac{1}{\Delta t}\,{}^{t}\dot{\mathbf{U}} - \frac{1}{\beta}\left(\frac{1}{2}-\beta\right)\,{}^{t}\ddot{\mathbf{U}}, $$

$$ {}^{t+\Delta t}\dot{\mathbf{U}} = {}^{t}\dot{\mathbf{U}} + (1-\gamma)\Delta t\,{}^{t}\ddot{\mathbf{U}} + \gamma\,{}^{t+\Delta t}\dot{\mathbf{U}}, $$

$$ {}^{t+\Delta t}\mathbf{U} = {}^{t}\mathbf{U} + \mathbf{u}. $$

Then the equilibrium iterations are performed with $\mathbf{K}^*$ updated with (3.50) and $\mathbf{F}^*$ updated by (3.51). The time integration algorithm is unconditionally stable for $2\beta \geq \gamma \geq 1/2$. For

other combinations the algorithm may be conditionally stable or unconditionally unstable. The combination $\beta = 1/4$, $\gamma = 1/2$, known as *trapezoidal rule*, leads to a second order accuracy in time unconditionally stable and to a maximum dissipation of the higher energy modes, usually creations of the discretization process [3]. We will use this combination in chapter 5.

## 3.5 Numerical procedures

The finite element method is accompanied by a large number of numerical procedures such as: numerical integration, numerical algorithms for solving nonlinear problems, methods for solving a linear system and procedures for solving eigenvalue problems as in vibrations analysis. In this section we mention briefly some of these methods which play an important role in the analysis of the diaphragm problem. Since we will use the program NIKE3D [4], we limit our presentation to numerical methods related to this code. The program is described briefly in section 5.2. In NIKE3D the following shape functions are used for displacement field modeling

$$\phi_i = \frac{1}{8}(1 - \xi_i\xi)(1 - \eta_i\eta)(1 - \zeta_i\zeta), \qquad \xi, \eta, \zeta \in [-1, 1], \tag{3.53}$$

where $\xi_i, \eta_i, \zeta_i$ are the local coordinates of the node $i$ as is shown in Figure 3.1. For the relative volume $\Theta$ and internal pressure $P$ a constant discontinuous functions are used for both variables.

$$\boldsymbol{\psi} = \begin{bmatrix} \psi & 0 & 0 \\ 0 & \psi & 0 \\ 0 & 0 & \psi \end{bmatrix}, \qquad \psi = 1.$$

The matrices from sections 3.3 and 3.4 are evaluated numerically. The procedure is a $2\times2\times2$ Gauss-type integration. Here we distinguish two types of integrals: volume integrals and surface integrals. A volume integral on the element $e$ is calculated as follows

$$\int_{\Omega_e} f(x_1, x_2, x_3)\, d\Omega = \int_{-1}^{+1}\int_{-1}^{+1}\int_{-1}^{+1} f(\xi, \eta, \zeta) J_e\, d\xi d\eta d\zeta = \sum_{i=1}^{2}\sum_{j=1}^{2}\sum_{k=1}^{2} f(\xi_i, \eta_j, \zeta_k) J w_i w_j w_k,$$

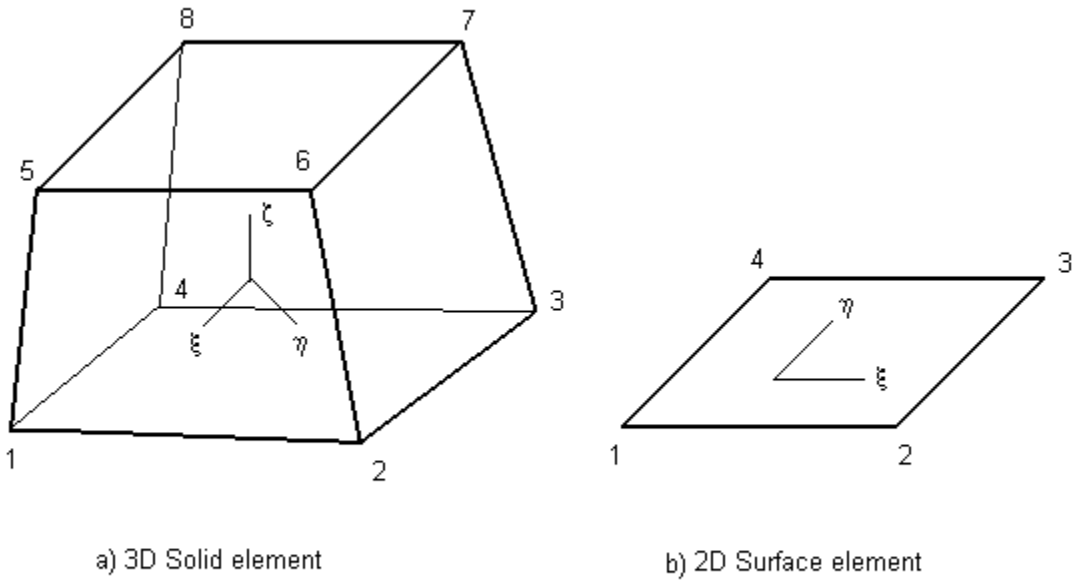


Figure 3.1: Three dimensional and two dimensional finite elements.

where $\xi_i, \eta_j, \zeta_k$ are the Gauss point coordinates and $w_i w_j w_k$ the Gauss weights and $J$ is the jacobian [58]

$$J = \begin{vmatrix} \frac{\partial x_1}{\partial \xi} & \frac{\partial x_1}{\partial \eta} & \frac{\partial x_1}{\partial \zeta} \\ \frac{\partial x_2}{\partial \xi} & \frac{\partial x_2}{\partial \eta} & \frac{\partial x_2}{\partial \zeta} \\ \frac{\partial x_3}{\partial \xi} & \frac{\partial x_3}{\partial \eta} & \frac{\partial x_3}{\partial \zeta} \end{vmatrix}.$$

The restriction of (3.53) to one of the faces of the solid element from Figure 3.1 b), for example $\zeta = 1$, is

$$\phi_i = \frac{1}{4}(1 - \xi_i \xi)(1 - \eta_i \eta), \qquad \xi, \eta, \zeta \in [-1, 1], \qquad i = 1, 4,$$

where $\xi_i, \eta_i$ are the local coordinates of the node $i$ as shown in Figure 3.1 b). An integral over the surface $\Sigma_e$ of an element $e$ becomes

$$\int_{\Sigma_e} f(x_1, x_2, x_3)\, d\Sigma = \int_{-1}^{+1} \int_{-1}^{+1} f(\xi, \eta) J_e \, d\xi d\eta = \sum_{i=1}^{2} \sum_{j=1}^{2} f(\xi_i, \eta_j) J w_i w_j, \tag{3.54}$$

where $\xi_i, \eta_j$ are the Gauss point coordinates and $w_i w_j$ the Gauss weights [58]. The surface jacobian $J$ is defined [1]

$$J = \left| \frac{\partial \boldsymbol{x}}{\partial \xi} \times \frac{\partial \boldsymbol{x}}{\partial \eta} \right| = \sqrt{EG - F^2}, \tag{3.55}$$

in which

$$E = \frac{\partial \boldsymbol{x}}{\partial \xi} \cdot \frac{\partial \boldsymbol{x}}{\partial \xi}, \qquad F = \frac{\partial \boldsymbol{x}}{\partial \xi} \cdot \frac{\partial \boldsymbol{x}}{\partial \eta}, \qquad G = \frac{\partial \boldsymbol{x}}{\partial \eta} \cdot \frac{\partial \boldsymbol{x}}{\partial \eta}.$$

The unit normal to the surface of the element $e$ is

$$\boldsymbol{n} = \frac{1}{J} \left( \frac{\partial \boldsymbol{x}}{\partial \xi} \times \frac{\partial \boldsymbol{x}}{\partial \eta} \right).$$

### 3.5.1 Nonlinear iterative algorithm

Solving equation (3.49) implies calculation of the tangent stiffness matrix $\mathbf{K}_T$ at every iteration, method called *full Newton-Raphson*. This is very expensive in the finite element analysis and therefore a modified procedure is usually used. One way is to use the tangent matrix from the first time step. This method is called the *initial stress method* and it usually leads to more iterations as the solution advances in time. The program NIKE3D uses a combination between these two methods called *modified Newton-Raphson* or *quasi Newton*. In this case the tangent stiffness matrix is formed at the beginning of the time step and it is kept constant during the equilibrium iterations [12]. In NIKE3D the iterative algorithm involves two steps

- Line searches.
- Stiffness update.

In the line search algorithm initially the displacements are updated with

$${}^{t+\Delta t}\mathbf{U} = {}^{t}\mathbf{U} + s^k \mathbf{u}^k,$$

where $s^k$ is a parameter between 0 and 1 that is determined iteratively by a line search procedure [3]. Equilibrium iterations are performed by solving (3.49) for $\mathbf{u}^k$. Convergence is

checked by using a displacement and the energy norm [12][3].

$$\frac{||\mathbf{u}^k||}{u_{max}} \leq \epsilon_d, \qquad \frac{(\mathbf{u}^k)^T \ {}^{t+\Delta t}\mathbf{Q}^k}{(\mathbf{u}^0)^T \ {}^{t+\Delta t}\mathbf{Q}^0} \leq \epsilon_e, \qquad {}^{t+\Delta t}\mathbf{Q} = {}^{t+\Delta t}\mathbf{F}^{ext} - \mathbf{F}^{int}({}^{t}\mathbf{U}),$$

where $\epsilon_d$ and $\epsilon_e$ are the tolerance for the displacement and energy norm respectively. Divergence is determined by a comparison of residual norms

$$\| \ {}^{t+\Delta t}\mathbf{Q}^0\| < \| \ {}^{t+\Delta t}\mathbf{Q}^k\|.$$

If convergence is not attained and the solution is not divergent, the displacements are updated by

$${}^{t+\Delta t}\mathbf{U}^k + 1 = \ {}^{t+\Delta t}\mathbf{U}^k + s^k\mathbf{u}^k,$$

and the iterations continue. When the solution diverges or convergence is not achieved after a number of iterations, the tangent stiffness matrix $\mathbf{K}_T$ is reformed using the current estimated geometry and the equilibrium iterations continue. The value of $s^k$ is found by iteration such that [41][3]

$$(\Delta\mathbf{U}^k)^T \ {}^{t+\Delta t}\mathbf{Q}^k \rightarrow 0, \qquad \Delta\mathbf{U}^k = \ {}^{t+\Delta t}\mathbf{U}^k - \ {}^{t+\Delta t}\mathbf{U}^{k-1}.$$

To update the stiffness matrix in NIKE3D four methods are implemented:

- Broyden's first method
- Davidon
- Davidon-Fletcher-Powell
- Broyden-Fletcher-Goldfarb-Shano (BFGS).

According to [28] these methods involving a line search are slightly more expensive in the computation but lead to a more stable program. Details of these methods can be followed in [39]. For our purpose we have used the BFGS method. In the NIKE3D program, the BFGS method follows the implementation proposed by Matthies and Strang [41]. Based on their algorithm, the inverse tangent stiffness matrix is updated by

$$(\mathbf{K}_T^k)^{-1} = \left[\mathbf{I} + \boldsymbol{w}^k\left(\boldsymbol{v}^k\right)^T\right](\mathbf{K}_T^{k-1})^{-1}\left[\mathbf{I} + \boldsymbol{v}^k\left(\boldsymbol{w}^k\right)^T\right],$$

where $\boldsymbol{v}^k$ and $\boldsymbol{w}^k$ are vectors defined as follows

$$\boldsymbol{\delta}^k = \Delta \boldsymbol{U}^{k-1}, \quad \boldsymbol{\gamma}^k = {}^{t+\Delta t}\mathbf{Q}^{k-1} - {}^{t+\Delta t}\mathbf{Q}^k,$$

$$\boldsymbol{v}^k = {}^{t+\Delta t}\mathbf{Q}^k - {}^{t+\Delta t}\mathbf{Q}^{k-1}\left[1 + \left(\frac{(\Delta \boldsymbol{U}^k)^T \boldsymbol{\gamma}^k}{(\boldsymbol{\delta}^k)^T \, {}^{t+\Delta t}\mathbf{Q}^{k-1}}\right)^{1/2}\right], \qquad \boldsymbol{w}^k = \frac{1}{(\boldsymbol{\delta}^k)^T \boldsymbol{\gamma}^k}\boldsymbol{\delta}^k.$$

One of the advantages of using this algorithm is that the determinant of $\mathbf{K}_T$ and therefore the change in the condition number of $\mathbf{K}_T$ can be easily computed in order to control the updates, especially in the situations when $\mathbf{K}_T$ becomes nearly singular and the condition number very large [41]. All the methods mentioned before for solving the nonlinear equations are in fact algorithms for minimization for convex problems [39]. In our situation the potential deformation energy is the function which needs to be minimized in order to find the solution. As long as the potential deformation energy remains strictly convex, i.e. a positive definite function, all those methods will converge. The methods will fail when the energy is no longer a convex function. In this case, a different approach is needed and the problem is still open [22]-[25]. For example, a particular case is the situation when the energy becomes semipositive definite, that is the buckling situation. However, for this particular case there are some algorithms that permit us to pass over this limit point, but only for some structures that can exibit either a *snap-through* or a *snap-back* phenomenon.

### 3.5.2 Arc-length method

When the load applied to a structure reaches a limit value, i.e. the point in the load/displacement space is in the neighbor of a limit or bifurcation point [53], as in Figure 3.2, the previous procedures fail to converge. In this case a special algorithm needs to be used in order to pass through that point. The theoretical basis for such algorithms was given by Riks in [45]. The approach described by Riks is theoretical rather than a practical one, and therefore, several authors have proposed practical algorithms based on Riks approach, for the finite element equations in the vicinity of a limit point: Chriesfield [19], Ramm [44], Schweizerhof [47], Riks-Wepmner [28]. These algorithms are known as *constant arc length* algorithms. The

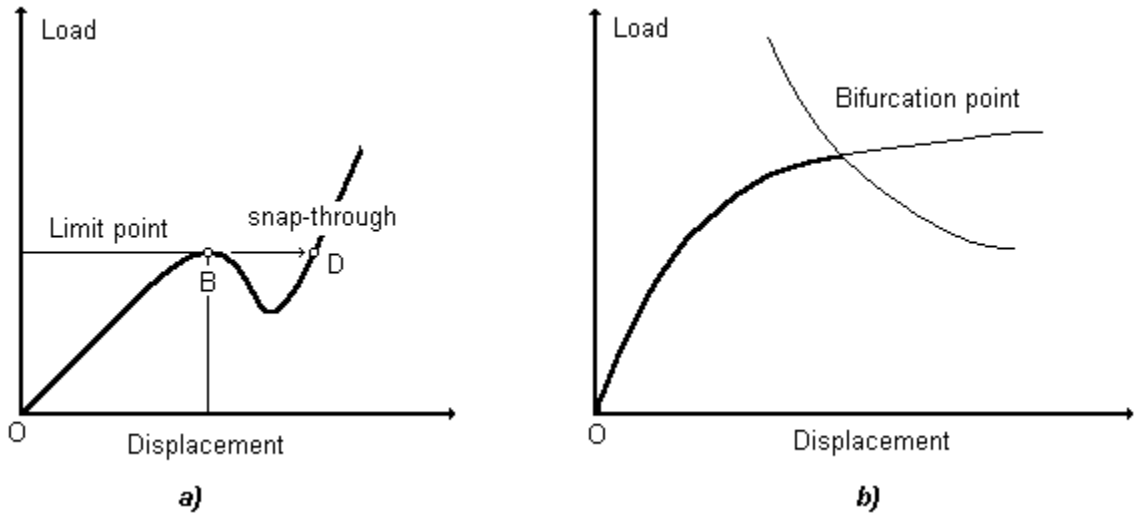


Figure 3.2: Limit point *a)*. Bifurcation point *b)*.

program NIKE3D uses the algorithm proposed by Riks-Wepmner [28][47]. Following [28], the incremental equilibrium equations (3.49) can be written as

$$\mathbf{K}_T\,\mathbf{u} = \lambda \mathbf{F}^{ext} - \mathbf{F}^{int},$$

where $\lambda$ is called the load factor parameter which has to be determined. This is done by adding a constraint equation

$$\mathbf{u}^T\mathbf{u} + \lambda^2 = s^2 = \text{const},$$

which represents the *length of the arc* in the load-displacement space. The load level is then split into three parts

$$\lambda = \lambda_m + \lambda_i + \Delta\lambda,$$

where $\lambda_m$ represents the load increment at the beginning of the load step, $\lambda_i$ represents the load level in the iteration $i$ and $\Delta\lambda_i$ the change in the load level in iteration $i$, which is determined through an iterative process. The increment in displacement is calculated

$$\mathbf{u} = \Delta\lambda_i \mathbf{u}^I + \mathbf{u}^{II}, \quad \mathbf{u}^I = \mathbf{K}_T^{-1}\,\mathbf{F}^{ext}, \quad \mathbf{u}^{II} = \mathbf{K}_T^{-1}\left[(\lambda_m - \lambda_i)\mathbf{F}^{ext} - \mathbf{F}^{int}\right], \tag{3.56}$$

where $\mathbf{u}^I$ represents the displacement due to the constraining condition and $\mathbf{u}^{II}$ represents the usual displacement increment. The linearization of the constraint equation yields

$$f(\mathbf{u},\lambda) = \mathbf{u}^T\mathbf{u} + \lambda^2 - s^2 = 0,$$

$$\frac{\partial f}{\partial \mathbf{u}}\mathbf{u} + \frac{\partial f}{\partial \lambda}\Delta\lambda + f(\mathbf{u},\lambda) = 0,$$

$$\boldsymbol{\gamma}^T\mathbf{u} + \alpha\Delta\lambda + f = 0, \qquad \boldsymbol{\gamma} = \frac{\partial f}{\partial \mathbf{u}}, \qquad \alpha = \frac{\partial f}{\partial \lambda},$$

and substituting (3.56) the following is obtained

$$\Delta\lambda = -\frac{f + \boldsymbol{\gamma}^T\mathbf{u}^{II}}{\alpha + \boldsymbol{\gamma}^T\mathbf{u}^I}.$$

Details of the calculations can be followed in [46].

## 3.6 Gateaux derivatives

The concept of Gateaux derivative used in Chapter 2 and Chapter 3 was used in conjunction to the idea that the deformation of a body can be regarded as a *map* between the reference (undeformed) and present (deformed) configuration of the body. Hence the definition of deformation gradient in section 2.1 requires the use of *derivative of a map*. This concept, which is the extension of the derivative of a function at a point, is defined by the Fréchet derivative of a map. Hence if $f$ is a map

$$f : \mathcal{X} \longrightarrow \mathcal{Y}$$

where $\mathcal{X}$ and $\mathcal{Y}$ are Banach spaces then $f$ is *differentiable* or Fréchet derivable at a point $x_0$ if there is a bounded linear map $Df(x_0)$ such that for each $\epsilon > 0$ there is a $\delta > 0$ such that $\| u \|_{\mathcal{X}} < \delta$ implies [40]

$$\| f(x + x_0) - f(x_0) - Df(x_0)\cdot u \|_{\mathcal{Y}} \leq \epsilon \| u \|_{\mathcal{X}} \tag{3.57}$$

where $\|\cdot\|_{\mathcal{X}}$, $\|\cdot\|_{\mathcal{Y}}$ defines a norm on $\mathcal{X}$, $\mathcal{Y}$ respectively. The equation (3.57) determines uniquely $Df(x_0)$. If $f$ and $g$ are two maps then the derivative Fréchet of the composite $g \circ f$ is defined by the chain rule [40]

$$D[(g \circ f)(x)] = Dg[f(x)] \cdot (Df(x) \cdot u) \tag{3.58}$$

The *directional derivative* of a map $f$ in the direction $u$ is defined as [40]

$$Df(x) \cdot u = D_u f(x) \cdot u = \frac{d}{d\varepsilon} \left[ f(x + \varepsilon u) \right]_{\varepsilon=0} \tag{3.59}$$

If (3.59) exists for all directions $u$ then $f$ is called *Gateaux differentiable at* $x$ [40]. The linearization of $f$ at $x_0$ is given by relation

$$L_{x_0} f(x) = f(x_0) + Df(x) \cdot (x - x_0)$$

To calculate the Gateaux derivatives used in this thesis we have used the formula (3.59) and the relation (3.58). For example to calculate $D_{\boldsymbol{\chi}} \boldsymbol{F} \cdot \boldsymbol{\upsilon}$ we proceed as below

$$D_{\boldsymbol{\chi}} \boldsymbol{F} \cdot \boldsymbol{\upsilon} = \frac{d}{d\varepsilon} \boldsymbol{F}(\boldsymbol{\chi} + \varepsilon \boldsymbol{\upsilon} \circ \boldsymbol{\chi}) \Big|_{\varepsilon=0} = \frac{d}{d\varepsilon} \left[ \frac{\partial(\boldsymbol{\chi} + \varepsilon \boldsymbol{\upsilon} \circ \boldsymbol{\chi})}{\partial \boldsymbol{X}} \right]_{\varepsilon=0} =$$

$$= D(\boldsymbol{\upsilon} \circ \boldsymbol{\chi}) = [\bigtriangledown \boldsymbol{\upsilon} \circ \boldsymbol{\chi}] \, \boldsymbol{F}, \qquad (\bigtriangledown \boldsymbol{\upsilon})_{ij} = \frac{\partial \upsilon_i}{\partial x_j}.$$

For simplicity of notation we have omitted the composition with $\boldsymbol{\chi}$ or in some cases with the inverse transformation $\boldsymbol{\chi}^{-1}$. We present below some Gateaux derivatives used in this thesis.

1.

$$D_{\boldsymbol{\chi}} \boldsymbol{F} \cdot \boldsymbol{\upsilon} = \bigtriangledown \boldsymbol{\upsilon} \boldsymbol{F}.$$

2.

$$D_{\boldsymbol{\chi}} J \cdot \boldsymbol{\upsilon} = J \operatorname{div} \boldsymbol{\upsilon}, \quad \operatorname{div} \boldsymbol{\upsilon} = \frac{\partial \upsilon_i}{\partial x_i}$$

3.

$$D_{\boldsymbol{\chi}}\overline{\boldsymbol{F}}\cdot\boldsymbol{v}=\Theta^{1/3}\left(-\frac{1}{3}\right)J^{-1/3}\frac{1}{J}D_{\boldsymbol{\chi}}J\cdot\boldsymbol{v}+\Theta^{1/3}J^{-1/3}D_{\boldsymbol{\chi}}\overline{\boldsymbol{F}}\cdot\boldsymbol{v}=$$

$$=\mathrm{dev}\left(\bigtriangledown\boldsymbol{v}\right)\overline{\boldsymbol{F}},\qquad\mathrm{dev}\left(\bigtriangledown\boldsymbol{v}\right)=\bigtriangledown\boldsymbol{v}-\frac{1}{3}\mathrm{div}\,\boldsymbol{v}\mathbf{1}$$

4.

$$D_{\boldsymbol{\chi}}\boldsymbol{C}\cdot\boldsymbol{v}=D_{\boldsymbol{\chi}}\boldsymbol{F}^{T}\cdot\boldsymbol{v}\boldsymbol{F}+\boldsymbol{F}^{T}D_{\boldsymbol{\chi}}\boldsymbol{F}\cdot\boldsymbol{v}=$$

$$=\boldsymbol{F}^{T}\mathrm{dev}\left[\left(\bigtriangledown\boldsymbol{v}\right)^{T}\right]\boldsymbol{F}+\boldsymbol{F}^{T}\mathrm{dev}\left[\bigtriangledown\boldsymbol{v}\right]\boldsymbol{F}=2\boldsymbol{F}^{T}\bigtriangledown^{s}\boldsymbol{v}\boldsymbol{F}$$

5.

$$D_{\boldsymbol{\chi}}W\cdot\boldsymbol{v}=\frac{\partial W}{\partial\boldsymbol{C}}D_{\boldsymbol{\chi}}\boldsymbol{C}\cdot\boldsymbol{v}=2\boldsymbol{F}^{T}\frac{\partial W}{\partial\boldsymbol{C}}\boldsymbol{F}\bigtriangledown^{s}\boldsymbol{v}$$

6.

$$\mathrm{GRAD}\;\boldsymbol{v}=\bigtriangledown\boldsymbol{v}\boldsymbol{F}$$

7.

$$D_{\boldsymbol{u}}J\cdot\boldsymbol{u}=J\mathrm{div}\,\boldsymbol{u}$$

8.

$$D_{\boldsymbol{u}}\boldsymbol{C}^{-1}\cdot\boldsymbol{u}=\frac{\partial\boldsymbol{C}^{-1}}{\partial\boldsymbol{C}}D_{\boldsymbol{u}}\boldsymbol{C}\cdot\boldsymbol{u}=-\boldsymbol{C}^{-1}\boldsymbol{C}^{-1}2\boldsymbol{F}^{T}\bigtriangledown^{s}\boldsymbol{v}\boldsymbol{F}=-\boldsymbol{F}^{-1}2\mathbf{I}\left(\boldsymbol{F}^{T}\right)^{-1}:\bigtriangledown^{s}\boldsymbol{v}$$

9.

$$D_{\boldsymbol{u}}\boldsymbol{S}\cdot\boldsymbol{u}=P\left(D_{\boldsymbol{u}}J\cdot\boldsymbol{u}\right)\boldsymbol{C}^{-1}+PJ\left(D_{\boldsymbol{u}}\boldsymbol{C}^{-1}\cdot\boldsymbol{u}\right)+2\frac{\partial^{2}\tilde{W}}{\partial\boldsymbol{C}\partial\boldsymbol{C}}\left(D_{\boldsymbol{u}}\overline{\boldsymbol{C}}\cdot\boldsymbol{u}\right)=$$

$$=J\boldsymbol{F}^{-1}P\left(\mathbf{1}\otimes\mathbf{1}\right)\left(\boldsymbol{F}^{T}\right)^{-1}:\bigtriangledown^{s}\boldsymbol{v}-\boldsymbol{F}^{-1}2\mathbf{I}\left(\boldsymbol{F}^{T}\right)^{-1}:\bigtriangledown^{s}\boldsymbol{v}+\boldsymbol{F}^{T}\mathbf{C}\boldsymbol{F}:\bigtriangledown^{s}\boldsymbol{v}=$$

$$=J\boldsymbol{F}^{-1}\left[P\left(\mathbf{1}\otimes\mathbf{1}-2\mathbf{I}\right)\right]\left(\boldsymbol{F}^{T}\right)^{-1}:\bigtriangledown^{s}\boldsymbol{v}+\boldsymbol{F}^{T}\mathbf{C}\boldsymbol{F}:\bigtriangledown^{s}\boldsymbol{v}$$